# $^{6}$Li and $^{6}$He elastic scattering from $^{12}$C and the effect of direct reaction couplings

N. Keeley*
*DSM/IRFU/SPhN CEA-Saclay, F-91191 Gif-sur-Yvette, France*

K. W. Kemper and O. Momotyuk
*Department of Physics, The Florida State University, Tallahassee, Florida 32306-4350, USA*

K. Rusek
*Department of Nuclear Reactions, The Andrzej Sołtan Institute for Nuclear Studies, Hoża 69, PL-00-681 Warsaw, Poland*
(Received 22 February 2008; published 22 May 2008)

Similarities in the $^{6}$Li and $^{6}$He elastic scattering from $^{12}$C at about 35 MeV/nucleon are manifested in the ability of an optical model potential that differs only in having a weaker imaginary strength for $^{6}$He than for $^{6}$Li to describe both data sets equally well. However, the weaker absorption seen in the $^{6}\mathrm{He} + {}^{12}\mathrm{C}$ data is counter to expectations of the effect of coupling to breakup channels, confirmed by continuum discretized coupled channels calculations. Coupled reaction channels calculations including couplings to the strongest transfer channels are also unable to account for this phenomenon.

DOI: 10.1103/PhysRevC.77.057601 PACS number(s): 25.60.Je, 24.10.Eq, 21.60.Gx, 27.20.+n

High quality exotic beam elastic scattering data that can be used to search for similarities and differences with previously measured stable beam data are beginning to become available. One comparison currently possible is between the systems $^{6}\mathrm{He} + {}^{12}\mathrm{C}$ [1] and $^{6}\mathrm{Li} + {}^{12}\mathrm{C}$ [2] where elastic scattering data are available for both systems at roughly 35 MeV/nucleon in energy. While it is possible to compare potential parameters derived from these data sets it is equally meaningful to compare the data directly when they are close in energy, as in the present case, to search for the physics determining the scattering.

We first display the data in the form of the ratio of the absolute cross section to that for Rutherford scattering versus center-of-mass (c.m.) angle, as is done traditionally for heavy ions, in Fig. 1(a). As can be seen, because of the different charges in the two systems a direct comparison of the data is not obvious. Figure 1(b) displays the absolute cross sections as a function of c.m. angle and now it becomes possible to see that the angular distributions have minima and maxima at roughly the same angles, albeit with a slight phase shift.

In Fig. 2 the data are displayed as absolute cross section versus momentum transfer of the two systems and it is immediately seen that the $^{6}$He and $^{6}$Li data have minima and maxima at the same transferred momenta. An immediate problem is observed at larger momentum transfers, where the $^{6}$He data have larger cross sections than those for $^{6}$Li, which is not what would be *a priori* expected. At larger momentum transfers, the elastic scattering begins to be dominated by the absorptive imaginary potential which produces the almost straight line decrease seen in the extensive $^{6}$Li data. Since the breakup threshold for $^{6}$He (0.973 MeV) is smaller than that for $^{6}$Li (1.47 MeV) a larger absorptive potential would be expected for $^{6}$He and hence its cross section would be smaller than that for $^{6}$Li as the transferred momentum increases. The present work explores possible explanations for the unexpectedly large $^{6}$He cross section through a series of coupled reaction channels (CRC) calculations performed with the code FRESCO [3] that explicitly include breakup and transfer channels.

The effect of projectile breakup on elastic scattering is now pretty well understood. At high enough bombarding energies, where Coulomb effects are negligible, it can be simulated in optical model (OM) calculations by a dynamic polarization potential with a repulsive real part and much weaker imaginary part [4]. The continuum discretized coupled channels (CDCC) method has proved to be a good technique to study couplings between breakup and elastic channels. The $^{6}\mathrm{He} + {}^{12}\mathrm{C}$ elastic scattering data of Lapoux *et al.* [1] have been studied using this method by different authors [4–6]. All these analyses led to a strong underestimation of the differential cross section for scattering angles larger than 15° in the center-of-mass frame. Matsumoto *et al.* [5] interpreted this effect as evidence of halo effects in $^{6}$He. In this work we perform a simultaneous analysis of both scattering systems, $^{6}\mathrm{He} + {}^{12}\mathrm{C}$ at 230 MeV and $^{6}\mathrm{Li} + {}^{12}\mathrm{C}$ at 210 MeV using the CDCC method to study in a consistent way the role of projectile breakup and its effect on elastic scattering.

Moro *et al.* [7] have shown that the structure of the three-body nucleus $^{6}$He can be approximated by a two-body dineutron model if the dineutron-alpha binding energy is set to 1.6 MeV. Since the two-body cluster structure of $^{6}$Li is well established, the two scattering systems may be investigated with the CDCC method using the same input parameters. In our CDCC calculations all the diagonal and coupling potentials were derived from empirical $d + {}^{12}\mathrm{C}$ and $\alpha + {}^{12}\mathrm{C}$ optical model potentials describing elastic scattering data at similar $E/A$ energies. For the deuteron the potential "série 2" of Duhamel *et al.* [8] was used while for the $\alpha + {}^{12}\mathrm{C}$ we

*Permanent address: Department of Nuclear Reactions, The Andrzej Sołtan Institute for Nuclear Studies, Hoża 69, PL-00-681 Warsaw, Poland.

 

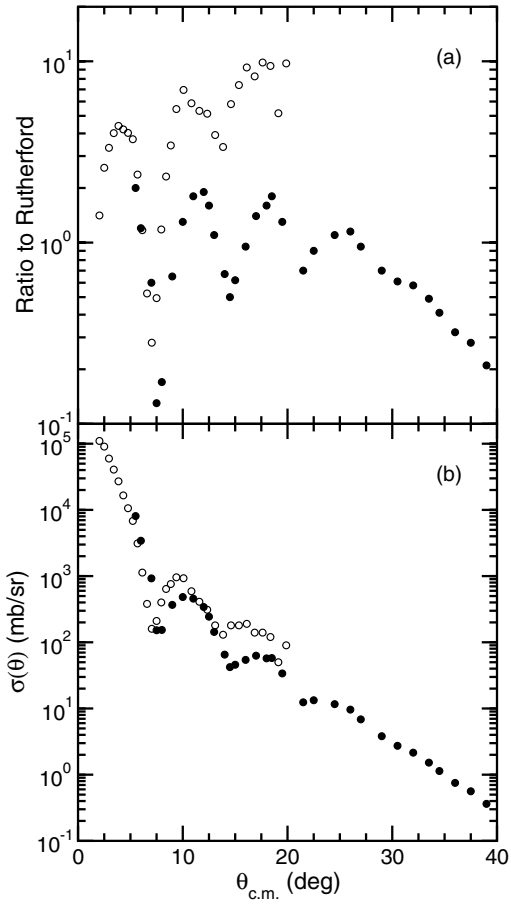


FIG. 1. Comparison of $^{6}$He (open circles) and $^{6}$Li (filled circles) elastic scattering cross sections from $^{12}$C at laboratory energies of 230 MeV and 210 MeV, respectively, as ratio to Rutherford (a) and absolute (b) cross sections as a function of center of mass scattering angle. The data are from Lapoux *et al*. [1] and Nadasen *et al*. [2].

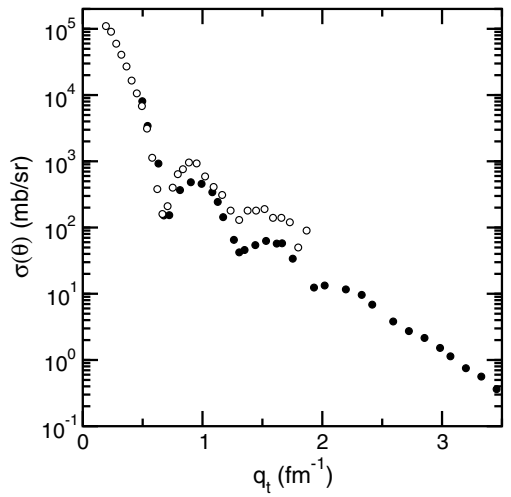


FIG. 2. Comparison of $^{6}$He (open circles) and $^{6}$Li (filled circles) elastic scattering cross sections from $^{12}$C at laboratory energies of 230 MeV and 210 MeV, respectively, as a function of transferred momentum.

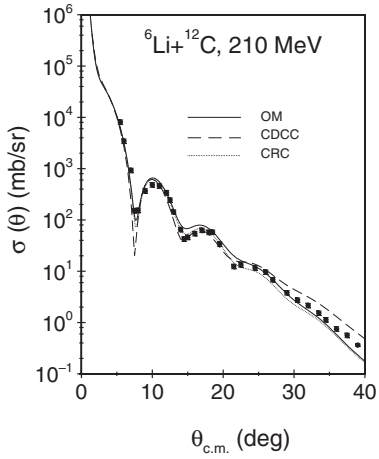


FIG. 3. Results of model calculations for $^{6}$Li + $^{12}$C elastic scattering. Data from Nadasen *et al*. [2].

took the potential proposed by Lapoux *et al*. [1] at $E/A = 34.75$ MeV.

For $^{6}$He we used the dineutron model of Moro *et al*. [7] while for $^{6}$Li we used the cluster model described in Pakou *et al*. [9], with the model space extended to about 17 MeV above the breakup threshold. The results of the calculations are presented in Figs. 3 and 4 by the dashed curves. For $^{6}$Li + $^{12}$C, the elastic scattering data are well described by the calculations with no free parameter. At angles larger than 25° the calculations slightly overestimate the data, suggesting that other direct processes, e.g., transfer reactions, should be included in the calculations. For $^{6}$He, the calculations strongly underestimate the data at angles larger than 10°. This effect could be compensated for by the introduction of a free parameter, a renormalization factor for the input imaginary potentials, $N_i = 0.5$. In summary, our consistent CDCC analysis of $^{6}$He, $^{6}$Li + $^{12}$C elastic scattering data has shown that the $^{6}$He data could not be described with an imaginary potential similar to that for $^{6}$Li.

The conclusion drawn from the CDCC calculations of the different $W$ strengths for both projectiles was confirmed by

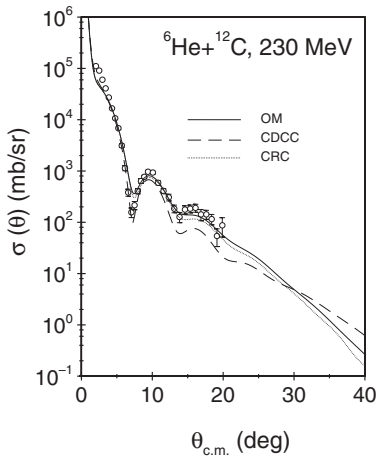


FIG. 4. Results of model calculations for $^{6}$He + $^{12}$C elastic scattering. Data from Lapoux *et al*. [1].

TABLE I. Calculated cross sections for different transfer channels.

| Channel | $Q_{gg}$ (MeV) | $\sigma_{\mathrm{DWBA}}$ (mb) |
|---|---|---|
| $^{12}$C($^{6}$Li, $^{5}$Li)$^{13}$C | −0.72 | 8.11 |
| $^{12}$C($^{6}$Li, $^{5}$He)$^{13}$N | −2.65 | 5.74 |
| $^{12}$C($^{6}$Li, $^{7}$Li)$^{11}$C | −11.47 | 4.70 |
| $^{12}$C($^{6}$Li, $^{7}$Be)$^{11}$B | −10.35 | 4.20 |
| $^{12}$C($^{6}$Li, $\alpha$)$^{14}$N | +8.80 | 0.03 |
| $^{12}$C($^{6}$Li, $^{8}$Be)$^{10}$B | −2.91 | 0.02 |
| $^{12}$C($^{6}$He, $^{5}$He)$^{13}$C | +3.08 | 13.36 |
| $^{12}$C($^{6}$He, $\alpha$)$^{14}$C | +12.25 | 0.01 |

an optical model analysis of the elastic scattering data. In the analysis we used optical model potentials of the standard form:

$$U(r) = V_C(r) - V(r) - iW(r), \tag{1}$$

with the nuclear part of Woods-Saxon shape:

$$V(r) = V_0(1 + \exp[(r - R_r)/a_r])^{-1}, \tag{2}$$

$$W(r) = W(1 + \exp[(r - R_w)/a_w])^{-1}. \tag{3}$$

We can describe very well both angular distributions with the same parameter set: $V_0 = 100$ MeV, $R_r = 3.08$ fm, $a_r = 0.85$ fm, $R_w = 3.78$ fm, $a_w = 0.75$ fm, the only difference being in the strength of the imaginary part, $W$: for $^{6}$Li $W = 38$ MeV while for $^{6}$He $W = 30$ MeV. The results of the calculations are plotted in Figs. 3 and 4 as the solid curves.

The different strengths of the imaginary potential for $^{6}$Li and $^{6}$He could be caused by transfer channels. An inspection of the ground state to ground state $Q$ values ($Q_{gg}$) suggests that transfer reactions induced by $^{6}$Li on $^{12}$C are better matched and thus should proceed with larger cross sections than reactions induced by $^{6}$He. This could explain the larger $W$ for $^{6}$Li. To test this hypothesis we performed a series of distorted wave Born approximation (DWBA) calculations for different transfer reactions.

The entrance channel optical model potentials used the parameters listed above. For exit channels leading to unbound isotopes of helium and lithium, $^{5}$He and $^{5}$Li, the optical potentials were calculated using the single-folding technique from a global $n$, $p$ target [10] and the $\alpha$-$^{12}$C optical potentials [1] used in our CDCC calculations. The wave functions of the $^{5}\mathrm{He} = \alpha + n$ and $^{5}\mathrm{Li} = \alpha + p$ ground states were generated in resonant continuum bins, as explained in [11]. The same binding potential [12] was used for both unbound nuclei. For $^{7}\mathrm{Li} + {}^{11}\mathrm{C}$, $^{7}\mathrm{Be} + {}^{11}\mathrm{B}$, and $^{8}\mathrm{Be} + {}^{10}\mathrm{Be}$ we used the same optical potential as in the entrance channel while for $\alpha + {}^{14}\mathrm{N}$ the global potential of Nolte *et al.* [13] was employed. Spectroscopic factors were taken from Refs. [14–20].

The results are listed in Table I. For one nucleon stripping reactions induced by $^{6}$Li we found that the strongest transitions are to the ground states of the residual nuclei and to the $5/2^{+}$ excited states placed at 3.55 MeV in $^{13}$N and at 3.85 MeV in $^{13}$C. The values listed in Table I are the sums for the two transitions. For one nucleon pickup, because of the highly negative $Q_{gg}$ values, the most pronounced transitions are to the ground states of the final nuclei. In the case of the $^{12}$C($^{6}$Li, $\alpha$) reaction, we took into account transitions to the ground state of $^{14}$N as well as to the two excited states, $3^{+}$ at 6.45 MeV and $5^{+}$ at 8.96 MeV, strongly excited in the low energy experiment of Mendez *et al.* [17]. For reactions induced by $^{6}$He, the strongest channel found in the calculations was one-neutron stripping leading to the ground and 3.85 MeV excited states of $^{13}$C. The cross section for two neutron transfer was found to be very small, in contrast to the low energy studies of DeYoung *et al.* [21] with a bismuth target. All the angular distributions are forward peaked, with rather small cross sections at scattering angles where the elastic cross sections significantly differ.

The strongest transfer channels were included in coupled reaction channels (CRC) calculations in order to see their effect on the elastic scattering. The results are plotted as the dotted curves in Figs. 3 and 4. The effect is similar for both projectiles: inclusion of transfer channels reduces the differential cross section for elastic scattering at angles larger than 10°. This could be compensated for by a reduction of the imaginary part of the entrance channel optical model potential. In other words, transfer reactions are responsible for removing flux from the entrance channel, but this effect is similar for both projectiles and does not explain the large difference in $W$ observed in the CDCC and OM analyses.

In conclusion, we have studied the elastic scattering of $^{6}\mathrm{Li} + {}^{12}\mathrm{C}$ and $^{6}\mathrm{He} + {}^{12}\mathrm{C}$ at similar energies high above the Coulomb barrier. Optical model calculations showed that the data could be described with potentials that differ only in the strength of the imaginary part, which is stronger for $^{6}$Li than for $^{6}$He. CDCC calculations including the effects of projectile breakup could not explain this phenomenon; detailed CRC calculations including all the strongest transfer channels also failed to explain it. We therefore find that the effect of breakup couplings is as expected, i.e., greater absorption for $^{6}$He than for $^{6}$Li, confirming that the larger elastic scattering cross section for $^{6}\mathrm{He} + {}^{12}\mathrm{C}$ is not explained by these couplings, in fact quite the contrary. This result agrees with Matsumoto *et al.* [4,5] who, using a four-body CDCC model, found that to describe the $^{6}\mathrm{He} + {}^{12}\mathrm{C}$ data they had to reduce the absorption of their bare potential compared to that expected from the systematics of previous $^{6}\mathrm{Li} + {}^{12}\mathrm{C}$ analyses [5]. Comparing dynamic polarization potentials derived from their four-body CDCC and an unmodified three-body CDCC dineutron model they found that the real parts were similar while the four-body CDCC gave a more absorptive imaginary part [4]. Thus, our calculation if anything underestimates the absorption due to breakup of $^{6}$He, although the modified dineutron model [7] used here will give a result closer to the four-body calculations than the basic model used in the comparisons of Ref. [4]. We further conclude that the observed difference in imaginary potentials could not be explained by inclusion of the strongest transfer channels.

N.K. gratefully acknowledges support from a European Commission Marie Curie Intra-European Actions Grant, Contract No. MEIF-CT-2005-010158. The work of K.W.K and O.M. was supported by the US National Science Foundation.

[1] V. Lapoux *et al*., Phys. Rev. C **66**, 034608 (2002).
[2] A. Nadasen *et al*., Phys. Rev. C **37**, 132 (1988).
[3] I. J. Thompson, Comput. Phys. Rep. **7**, 167 (1988).
[4] T. Matsumoto *et al*., Phys. Rev. C **70**, 061601(R) (2004).
[5] T. Matsumoto *et al*., Nucl. Phys. **A738**, 471 (2004).
[6] M. Rodriguez-Gallardo *et al*., arXiv:0710.0769v1 [nucl-th].
[7] A. M. Moro, K. Rusek, J. M. Arias, J. Gómez-Camacho, and M. Rodriguez-Gallardo, Phys. Rev. C **75**, 064607 (2007).
[8] G. Duhamel *et al*., Nucl. Phys. **A174**, 485 (1971).
[9] A. Pakou *et al*., Phys. Lett. **B633**, 691 (2006).
[10] R. L. Varner *et al*., Phys. Rep. **201**, 57 (1991).
[11] K. Rusek, L. Giot, and P. Roussel-Chomaz, Eur. Phys. J. A **32**, 159 (2007).
[12] J. Bang and C. Gignoux, Nucl. Phys. **A313**, 119 (1976).
[13] M. Nolte, H. Machner, and J. Bojowald, Phys. Rev. C **36**, 1312 (1987).
[14] S. Cohen and D. Kurath, Nucl. Phys. **A101**, 1 (1967).
[15] O. F. Nemets *et al*., *Nucleon Clusters in Atomic Nuclei and Many-Nucleon Transfer Reactions* [in Russian] (Ukrainian Academy of Science, Institute for Nuclear Research, Kiev, 1988).
[16] M. B. Tsang, J. Lee, and W. G. Lynch, Phys. Rev. Lett. **95**, 222501 (2005).
[17] A. J. Mendez *et al*., Phys. Rev. C **51**, 651 (1995).
[18] S. Yu. Mezhevych *et al*., Nucl. Phys. **A753**, 13 (2005).
[19] R. J. Peterson and J. J. Hamill, Phys. Rev. C **22**, 2282 (1980).
[20] F. Ajzenberg-Selove, Nucl. Phys. **A523**, 1 (1991).
[21] P. A. DeYoung *et al*., Phys. Rev. C **71**, 051601(R) (2005).